EurJIC
European Journal of Inorganic Chemistry
ChemPubSoc Europe

DOI:10.1002/ejic.201500365

Pt, Pd and Hg Complexes with Potentially Tridentate Telluroether Ligands

Lars Kirsten,[a] Vania D. Schwade,[b] Lars Selter,[a] Adelheid Hagenbach,[a] Paulo C. Piquini,[c] Ernesto Schulz Lang,*[b] and Ulrich Abram*[a]

Keywords: Tellurium / Ligand design / Palladium / Platinum / Mercury / Solid-state structures

N-[3-(Phenyltellanyl)propyl]picolinamide (HL1) or *N*-[*N''*,*N''*-methyl(phenyl)aminothiocarbonyl]-*N'*-[3-(phenyltellanyl)propyl]benzamidine (HL2) react with equivalent amounts of $PtCl_2$ or $PdCl_2$ with formation of neutral [MCl(L1-κ*N*,*N'*,*Te*)] or [MCl(L2-κ*S*,*N*,*Te*)] chelates. A corresponding reaction of HL2 with $HgCl_2$ results in the formation of [$HgCl_2$(HL2-κ*S*,*Te*)]. Treatment of [PtCl(L1-*N*,*N'*,*Te*)] with elemental iodine results in the exclusive oxidation of the metal ion and the platinum(IV) complex [PtI_3(L1-κ*N*,*N'*,*Te*)] could be isolated in reasonable amounts. A decomposition of the tellurium-containing ligand and the formation of [PdI_2($(PhTeI)_2$)] was observed during a similar procedure with the corresponding palladium complex. The bonding situation inside the latter compound was analyzed through density functional theory calculations.

Introduction

A large number of metal complexes with ether, thioether, or selenoether ligands is known,[1–5] and interest in the corresponding tellurium-containing ligands has increased during the last decades. Monodentate, bidentate, and cyclic telluroethers have been synthesized, which show suitable complexation behavior, particularly for low-valent transition-metal ions.[3–10] The introduction of additional donor atoms such as N, O, P, S, or Se leads to hybrid telluroethers, which are more variable with regard to their coordination behavior and form stable complexes with more metal ions.[6,11] Reports on telluroethers containing two or more different donor groups in addition to tellurium such as the O,N,Te-ligands of Scheme 1 and their metal complexes are less common.[12–20] Frequently, amido groups such as those in compounds **1** and **2**, Schiff bases (compounds **3** and **4**) or the corresponding amines (compounds **5** and **6**) accompanied by phenolic groups are used as donor functionalities.

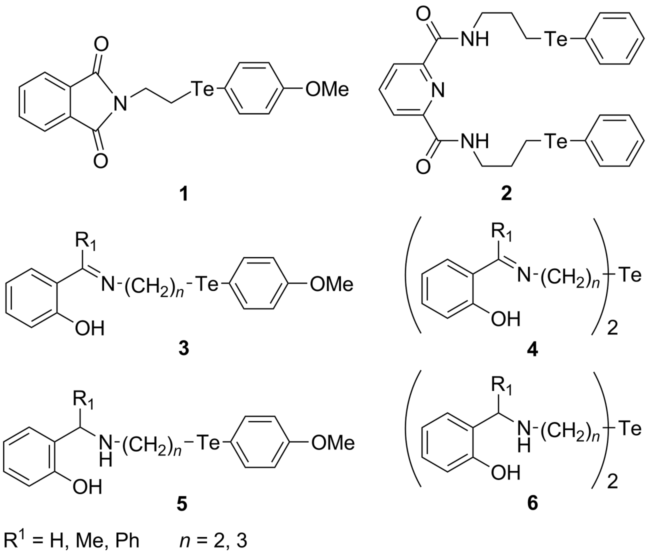

Scheme 1. Frequently used multidentate telluroether ligands.

The number of transition-metal ions used for coordination chemistry with the ligands shown in Scheme 1 is restricted to "tellurophilic ions" such as Co^{2+}, Pd^{2+}, Pt^{2+}, Ru^{2+}, and Hg^{2+}. Depending on the metal ion, telluroethers **1**–**6** can act as monoanionic tridentate chelators, as found in the majority of the structurally characterized Pd^{2+} and Pt^{2+} complexes. When deprotonation is not possible (as for ligand **1**), *N*,*Te*-coordination is observed for Pd^{2+} under conservation of a *cis*-$PdCl_2$ unit.[15] A specific feature of Schiff bases **3** is the influence of the size of the alkyl chain on the coordination modes of the ligands in a way that the

---

[a] Institute of Chemistry and Biochemistry, Freie Universität Berlin,
Fabeckstr. 34/36, 14195 Berlin, Germany
E-mail: ulrich.abram@fu-berlin.de
http://www.bcp.fu-berlin.de/chemie/chemie/forschung/InorgChem/agabram/index.html
[b] Departamento de Química, Laboratório de Materiais Inorgânicos, Universidade Federal de Santa Maria,
97105-900 Santa Maria, RS, Brazil
http://jararaca.ufsm.br/websites/lmi_english/index.htm
[c] Departamento de Física, Universidade Federal de Santa Maria,
97105-900 Santa Maria, RS, Brazil

Supporting information for this article is available on the WWW under http://dx.doi.org/10.1002/ejic.201500365.

ligands with ethylene bridges act as tridentate O,N,Te-donors, whereas monodentate tellurium coordination is observed for the propylene derivatives.[17] Corresponding Co^{2+} complexes show a high flexibility with respect to the established different coordination modes and coordination spheres, whereas Ru^{2+} metal ions are exclusively bidentate *N*,*Te*-coordinated under conservation of a [RuCl(*p*-cymene)] moiety.[17,21] An exception is ligand **4**, which acts as a monoanionic tridentate chelator for a Ru^{2+} ion under replacement of a *p*-cymene co-ligand.[16] Hg^{2+} complexes of the potentially tri- or pentadentate Schiff bases **3** and **4** are characterized by exclusive coordination of the soft Te donors by two such ligands to central $\{HgBr_2\}$ units.[16,17,22] Bidentate *N*,*Te*-coordination is observed for complexes with metals in their higher oxidation states such as Co^{3+}, Rh^{3+}, or Pt^{4+}.[23] The solid-state structures of some of the complexes show characteristic intermolecular secondary interactions between tellurium and chlorine atoms of adjacent molecules.[16,18,19,24–26]

Our interest focuses on the coordination chemistry of potentially tridentate telluroether ligands as building blocks for monomeric transition-metal complexes. Their spatial arrangement in the solid-state structures of the products may allow secondary interactions between tellurium and the metal ions and/or coordinated halido ligands. The used ligands are derived from (phenyltellanyl)propylamine, to which picoloyl (HL1) and thiocarbamoylbenzimidoyl units (HL2) were attached, respectively.

Results and Discussion

Reactions of (phenyltellanyl)propylammonium chloride with picolinoyl chloride or *N*-[*N′*,*N′*-methyl(phenyl)aminothiocarbonyl]benzimidoyl chloride in anhydrous acetonitrile or acetone gave the proligands HL1 and HL2 in good yields (Scheme 2). The addition of NEt_3 supports the reaction by the precipitation of $Et_3N{\cdot}HCl$.

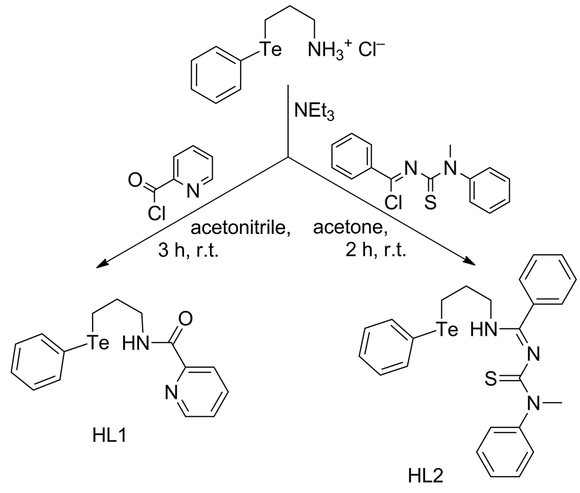

Scheme 2. Synthesis of HL1 and HL2.

Both products were obtained as viscous oils, which could not be solidified even after several chromatographic purification procedures. The obtained elemental analytical data were satisfactory in this context and the spectroscopic studies support the formation of the potentially tridentate ligands. ESI^+ mass spectra of the compounds show intense peaks for the molecular ions and/or the corresponding cluster ions with Na^+ and K^+, respectively. The ^{125}Te NMR signals appear at δ = 483 ppm (HL1) and 471 ppm (HL2), which is, as expected, in the same range as the signal of the starting compound $PhTe(CH_2)_3NH_3^+Cl^-$ (δ = 475 ppm) and other aryl alkyl telluroethers.[27]

Reactions of HL1 and HL2 with $PtCl_2$ or $PdCl_2$ resulted in the formation of [MCl(L)] complexes (Scheme 3). The products could be isolated as orange-red (complexes with $L1^-$) or brown (complexes with $L2^-$) solids. All these compounds contain the telluroethers as singly deprotonated, tridentate ligands. Single crystals of the products with HL1 could be obtained from recrystallization from CH_2Cl_2/MeOH or dimethyl sulfoxide (DMSO). The molecular structure of [PtCl(L1-κ*N*,*N′*,*Te*)] (**7**), which was obtained from a DMSO solution of the complex, is depicted in Figure 1. The molecular structure of the analogous palladium

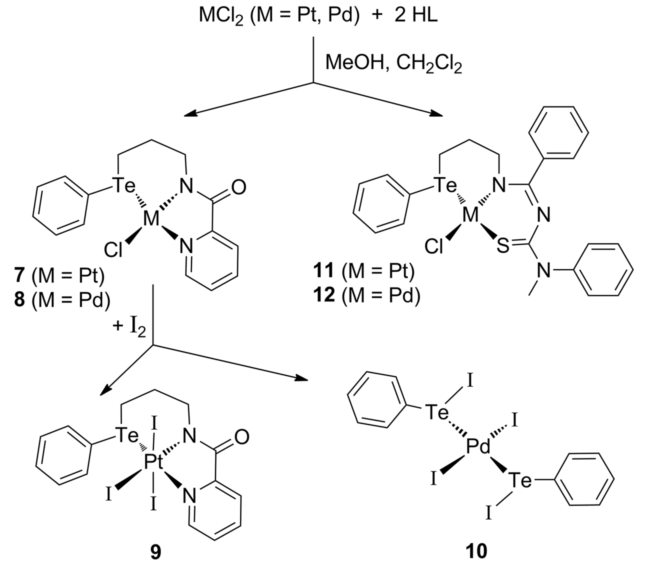

Scheme 3. Synthesis of Pt^{II} and Pd^{II} complexes with HL1 and HL2 and their reactions with iodine.

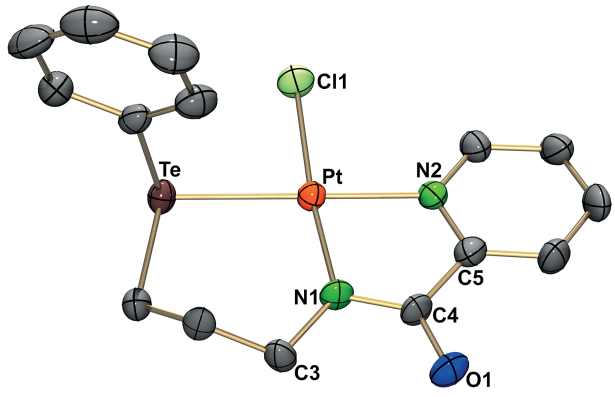

Figure 1. Molecular structure of **7**.[28] Hydrogen atoms are omitted for clarity.

complex is virtually the same, and no extra figure is shown. Selected bond lengths and angles are contained in Table 1. Differences in the crystal packing due to long-range interactions will be discussed below.

Table 1. Selected bond lengths [Å] and angles [°] in complexes containing $L1^-$ (M = Pt, Pd; X = Cl, I).

	7	8	9
M–X1	2.324(2)	2.337(2), 2.328(2) 2.329(2), 2.331(2)	2.599(1)
M–Te	2.526(1)	2.532(1), 2.526(1) 2.519(1), 2.528(1)	2.590(1)
M–N1	2.017(5)	2.012(5), 2.012(5) 2.026(6), 2.036(5)	2.06(1)
M–N2	2.059(6)	2.057(5), 2.072(5) 2.046(5), 2.067(5)	2.11(1)
M–I2			2.667(1)
M–I3			2.669(1)
N1–C4	1.343(9)	1.341(8), 1.357(9) 1.327(9), 1.330(9)	1.33(2)
C4–O1	1.256(8)	1.260(7), 1.251(8) 1.248(8), 1.244(7)	1.23(2)
X1–M–Te1	84.44(5)	85.39(5), 84.00(5) 84.48(5), 84.34(5)	83.17(4)
X1–M–N1	173.6(2)	174.6(2), 176.2(2) 174.9(2), 175.1(2)	174.8(3)
X1–M–N2	94.2(2)	94.7(2), 96.7(2) 95.6(2), 95.3(1)	96.9(3)
Te1–M–N1	100.6(2)	98.5(2), 98.6(2) 99.0(2), 99.6(2)	100.3(3)
Te1–M–N2	177.6(2)	179.4(1), 178.3(1) 179.4(1), 178.9(1)	177.0(3)
N1–M–N2	80.9(2)	81.4(2), 80.6(2) 80.9(2), 80.8(2)	79.4(4)
M–N1–C3	129.2(5)	131.5(4), 128.7(5) 129.1(6), 126.9(5)	124.9(9)
M–N1–C4	115.5(5)	114.5(4), 115.7(4) 115.1(4), 114.9(5)	115.5(9)
N1–C4–O1	127.4(7)	126.2(7), 125.9(6) 126.9(7), 126.6(6)	125(1)
N1–C4–C5	114.8(7)	115.6(5), 114.4(6) 115.2(6), 115.0(5)	115(1)

The platinum atom shows the expected square-planar coordination sphere. Slight distortions are observed due to the restricting bite angle of the five-membered chelate ring, which results in a N1–Pt–N2 angle of 80.9(2)°. Whereas the coordination plane consisting of the platinum atom and the atoms Cl1, N1, N2 and Te1 and the five-membered chelate ring are almost flat with a maximum deviation of 0.129(6) Å (for N1) and 0.012(8) Å (for C4 and C5), the alkyl chain of the six-membered chelate ring, as expected, cause a stronger deviation from planarity [0.494(8) Å for C2].

The molecular bonding situation in the corresponding palladium compound **8** is almost identical. Remarkable differences are, however, clear in the intermolecular packing scheme in the solid state. The unit cell of **8**·MeOH·1/2 H_2O contains four independent [PdCl(L1-κ*N*,*N*′,*Te*)] molecules, which results in the four values for each bond length and angle in Table 1.

The [PtCl(L1)] molecules **7** are arranged in dimeric units in the solid state by additional Pt···Te contacts of 3.7154(8) Å as visualized in Figure 2 (a). No further intermolecular interactions could be found for the solvent-free platinum complex, which was crystallized from DMSO. The formation of dimeric units was also observed for the analogous palladium complex **8**. Here, however, Pd···Pd contacts of 3.236(1) and 3.323(1) Å are responsible for the aggregation. These are supported by long-range Te···Cl contacts between 3.418(2) and 3.520(2) Å (red dashed lines in Figure 2, b). Each four of the resulting dimers are organized in short zigzag chains by additional weak Te···Cl contacts in the range between 3.850(2) and 4.223(2) Å (blue dashed lines in Figure 2, c). Finally the aggregates are organized into infinite chains. They are well separated from each other by the aromatic rings, which prevent them from further aggregation. The cocrystallized methanol and water molecules form weak hydrogen bonds with each other and the carbonyl oxygen atom of $L1^-$, but do not contribute to the intermolecular assembly of the complex molecules.

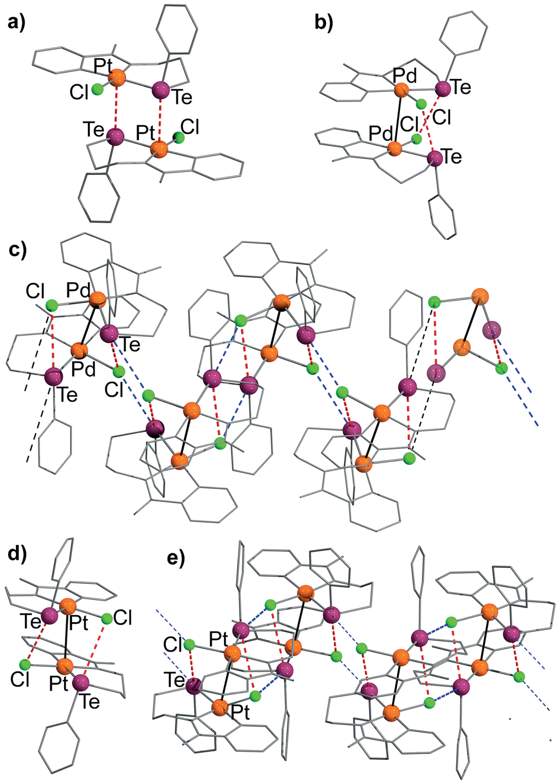

Figure 2. Intermolecular aggregation patterns of **7** and **8**.[28]

A similar bonding situation with structure-determining Te···Cl contacts of different lengths as has been described for the solid-state structure of the palladium complex **8**, has also been observed for the platinum compound, when this is crystallized from CH_2Cl_2/MeOH. Triclinic crystals (space group $P\bar{1}$) with an unusually large unit cell [a = 16.058(2), b = 18.527(2), c = 26.200(2) Å, α = 78.61(1), β = 84.69(1), γ = 63.92(1)°] contain eight symmetry-independent [PtCl(L1)] molecules in the asymmetric unit. They are organized as shown in Figure 2 (d and e). Basic dimeric units are formed, similar to the situation in **8**, by platinum–platinum interactions [3.232(2)–3.337(2) Å], which are supported by Te···Cl contacts between 3.421(1) and 3.623(1) Å. The resulting units are connected by another group of Te···Cl long-range interaction [3.762(2)–4.732(2) Å, blue dashed lines in Figure 2, e] to infinite zigzag chains.

Soft interactions between tellurium and electronegative atoms are not unusual in the chemistry of this element and frequently dominate the structural chemistry of organotellurium compounds by self-organization of smaller units to larger assemblies.[29–32] For coordination compounds with tellurium-containing ligands, however, such effects are less regarded. The present examples demonstrate that Te···Cl interactions can support weak metal–metal bonds and finally form dimeric units of certain stability. The ESI mass spectra of **7** and **8** demonstrate that dimeric assemblies exist not only in the solid-state structures of the complexes, but can also be transferred into the gas phase. This can be derived by the detection of ions of reasonable abundance (22 and 46 per cent of the base peak) at *m*/*z* 1218.8991 and 1040.7841, which can be assigned to the $[\{PtCl(L1)\}_2 + Na]^+$ (calcd. 1218.9063) and $[\{PdCl(L1)\}_2 + Na]^+$ (calcd. 1040.7837) ions. Mass peaks, which belong to fragments with more than two metal atoms, can also be assigned, but these are of lower intensity. NMR studies on **7** and **8** in DMSO do not give evidence for the existence of different species of the complexes in solution. The ^{125}Te spectrum shows, in each case, only one signal for the platinum and palladium complexes at 537 and 577 ppm, respectively. The ^{195}Pt signal of **7** appears at –3450 ppm.

A rough estimation of the long-range Te···Cl interactions in the solid-state structures of **7** and **8** can be made on the basis of an analysis of X-ray structural data of more than 500 organotellurium compounds with Te···X interactions.[33] In this study, a range of intermolecular Te···Cl interactions between 3.2 and 4.0 Å, with a mean value of 3.672 Å, has been identified. Thus, it may be concluded that, for the Pt and Pd complexes under study, the aggregation of the tetrameric units is the result of weak Te···Cl interactions, whereas their role in the formation of the polymeric chains is not clear.

The reaction of platinum(II) complex **7** with elemental iodine results in the exclusive oxidation of the central metal ion and the replacement of the Cl$^-$ ligand by I$^-$. The telluroether ligand remains untouched and the resulting octahedral Pt^{IV} complex $[PtI_3(L1)]$ (**9**) contains the tridentate L1$^-$ ligand together with three iodido ligands. The Pt–N and Pt–Te bonds are slightly longer than those in the Pt^{II} compound. Selected bond lengths and angles are contained in Table 1. An ellipsoid representation of the complex molecule is shown in Figure 3. Intermolecular Te···X or Te···M long-range interactions, which have been found for compounds **7** and **8**, do not play any role in the solid-state structure of compound **9**.

As expected, an analogous reaction of the palladium complex **8** with iodine results in completely different products. In this case, the attack is directed to the framework of the organic ligand and a number of decomposition products are formed, as can be concluded from the ^{125}Te NMR spectrum of the reaction mixture, which shows numerous signals.

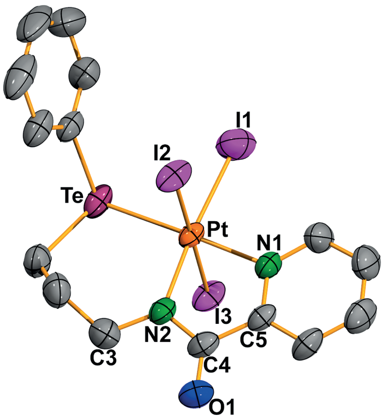

Figure 3. Molecular structure of complex **9**.[28] Hydrogen atoms are omitted for clarity.

Only one of the products, $[PdI_2(PhTeI)_2]$ (**10**), could be isolated in crystalline form and studied by X-ray crystallography. The molecular structure of this remarkable compound is shown in Figure 4 and selected bond lengths and angles are given in Table 2. The palladium(II) compound contains two phenyltellurenyl iodide ligands (PhTeI), which are products of the cleavage of the labile Te–C(aliphatic) bond in HL1. Free phenyltellurenyl iodide exists as a tetrameric aggregate with a central, almost planar Te$_4$ ring, which is formed by secondary Te···Te interactions between 3.153(1) and 3.181(1) Å.[34] Monomeric PhTeI building blocks are usually stabilized by donor ligands such as phosphines or thiones,[35–37] or by coordination to metal ions.[38,39]

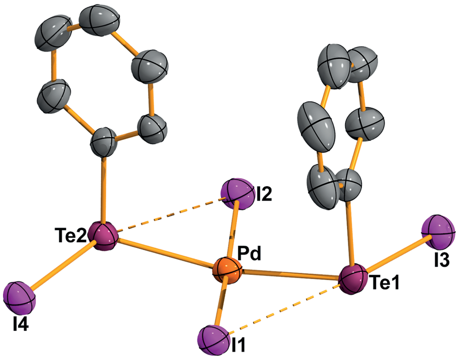

Figure 4. Molecular structure of complex **10**.[28] Hydrogen atoms are omitted for clarity.

Table 2. Selected bond lengths [Å] and angles [°] in **10**.

Pd–Te1	2.295(1)	Pd–Te2	2.583(1)
Pd–I1	2.599(1)	Pd–I2	2.595(1)
Te1–I3	2.721(1)	Te2–I4	2.739(1)
Te1···I1	3.335(1)	Te2···I2	3.267(1)
I1–Pd–Te1	79.90(4)	I1–Pd–Te2	100.17(4)
I1–Pd–I2	176.32(4)	I2–Pd–Te1	100.85(4)
I2–Pd–Te2	78.24(4)	Te1–Pd–Te2	166.47(4)
I1···Te1–I3	160.46(3)	I2–Pd···I4	161.40(3)

The square-planar coordination environment of the palladium atom in **10** is markedly distorted in that the two iodido ligands are bent towards the lone pairs of the tellurium atoms of the PhTeI ligands. This results in Te···I distances of 3.267(1) and 3.335(1) Å and may indicate interactions between these atoms, which finally strengthen the Pd–Te bonds. Similar findings have been reported recently for manganese and iron complexes.[38]

To verify the bonding properties of compound **10**, we performed a natural bond order analysis through density functional theory calculations. We first performed an optimization of the compound geometry, which led to a C_{2v} symmetry structure. The optimized atomic coordinates and infrared vibrational spectra are given in the Supporting Information. The higher point group symmetry of theoretically optimized structure in vacuo, as compared with that extracted from the X-ray diffraction data, has its origin in a twist angle between the two phenyl rings of 74° in the solid-state structure of the compounds, which is readily explained by packing effects. The experimentally determined bonding situation in the coordination sphere of the palladium atom is, however, well reproduced by the calculations. This also includes the experimentally detected deviations from an ideal square-planar coordination sphere with calculated I1–Pd–Te1 and I1–Pd–Te2 angles of 77.21 and 102.83°, respectively. This results in Te1···I3 (Te2···I2) distances of 3.36 Å.

Table 3 shows the calculated natural bond orders for selected pairs of atoms of the C_{2v} structure for compound **10**. The Te1–I1 (Te2–I2) bond orders, although almost three times smaller than those for Te1–I3 (Te2–I4), are still significant, showing the role played by these additional Te–I interactions in the stabilization of compound **10** as a whole and confirms similar conclusions drawn previously.[38] The resulting bonding situation can be visualized by looking at the electron localization function map of the PdTeI plane of the compound, as shown in Figure 5.

Table 3. Calculated natural bond order for selected pairs of atoms of compound **10**.

Pd–Te1	0.582	Te1–I1	0.281
Pd–I1	0.670	Te1–I3	0.760

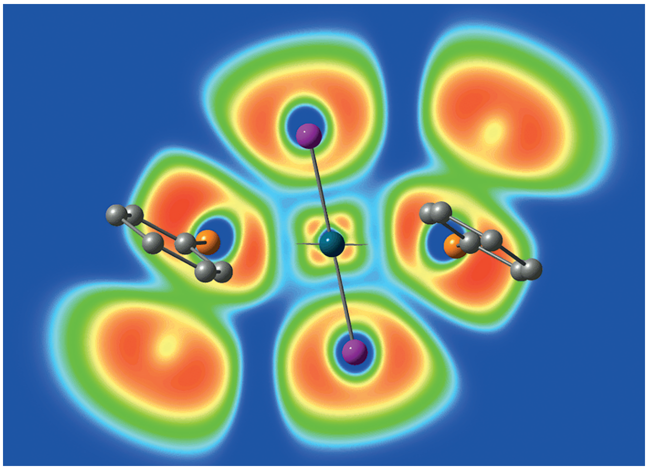

Figure 5. Electron localization function for compound **10**, calculated at a plane containing the Pd, Te, and I atoms.

A Bader analysis of compound **10** at a plane parallel to the Pd, Te, and I atoms, is shown in Figure 6. It can be seen that there is no saddle point of the electronic density between the Te1 and I1 (Te2 and I2) atoms. This result confirms the weak nature of the bond between these atoms, as compared with the Te2–I4 (Te1–I3) bonds, and complements the information given by the electron localization function given in Figure 5.

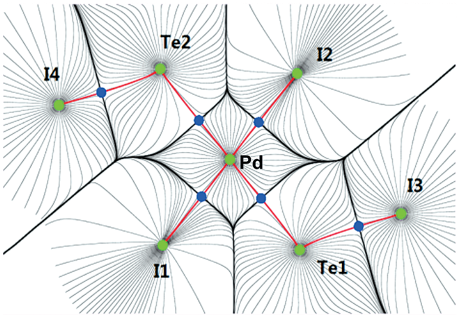

Figure 6. Bader analysis at a plane parallel to the Pd, Te, and I atoms of compound **10**. The black solid curves represent the vector field of the gradient of the electron density. The red lines show the molecular graph at the plane. The green and blue circles show the position of the maxima and saddles of the electronic distribution, respectively.

Reactions of $PtCl_2$ and $PdCl_2$ with ligand HL2 result in the formation of microcrystalline brown solids of composition [MCl(L2)]. These materials are readily soluble in DMSO and only moderately soluble in $CHCl_3$, CH_2Cl_2, and MeOH. Their infrared spectra show a significant bathochromic shift of the C=N band of the benzamidine unit from 1598 cm^{-1} in the uncoordinated HL2 to 1529 cm^{-1} in **11** and 1544 cm^{-1} in **12**. Such a shift is common for chelate formation with such ligands and goes along with π-electron delocalization within the six-membered chelate ring. Similar to the Pt^{II} and Pd^{II} complexes with $L1^-$, the ESI^+ mass spectra of compounds **11** and **12** also give evidence for an aggregation to dimeric units. Unfortunately, we did not obtain single crystals for these complexes. Thus, it is not clear whether the dimers are preformed in the solid state or which type of interactions are responsible for their formation.

Although we could not isolate pure products from attempted reactions between HL1 and $HgCl_2$, colorless crystals of [$HgCl_2$(HL2-κ*S*,*Te*)] (**13**) were obtained from a corresponding reaction with HL2 (Scheme 4). Unlike the situation in the platinum and palladium complexes, the ligand is not deprotonated in the mercury compound and coordinates only in a bidentate fashion through tellurium and sul-

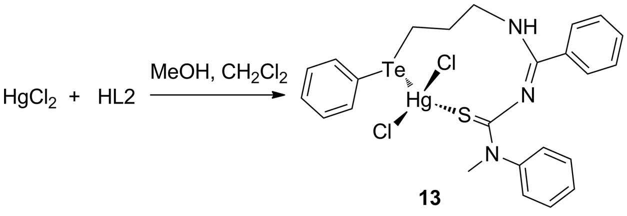

13

Scheme 4. Synthesis of [$HgCl_2$(HL2-κ*S*,*Te*)].

fur. These findings are easily explained with the favored tetrahedral coordination environment of the Hg^{2+} ion and the preferred coordination of the "soft" tellurium and sulfur donor atoms to the "soft" metal ion. Consequently, the central nitrogen donor atom remains protonated and uncoordinated. Attempts to enforce deprotonation of HL2 during the reaction with $HgCl_2$, with NEt_3 as supporting base, did not give tridentate coordination of $L2^{-}$, but resulted in decomposition of the telluroether and formation of elemental tellurium. The molecular structure of compound **13** is shown in Figure 7a; selected bond lengths and angles are given in Table 4.

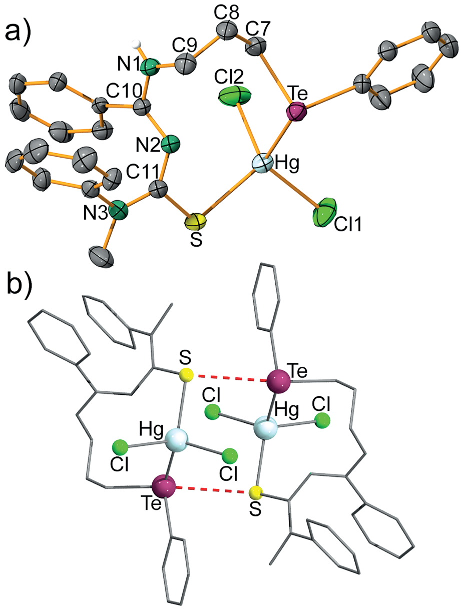

Figure 7. (a) Molecular structure of complex **13**.[28] Hydrogen atoms are omitted for clarity. (b) Dimerization of the molecules through Te···S long-range interactions.

Table 4. Selected bond lengths [Å] and angles [°] in **13**.

Hg–Te	2.751(1)	Hg–S	2.487(1)
Hg–Cl1	2.482(1)	Hg–Cl2	2.550(1)
Te–C7	2.155(4)	S–C11	1.721(4)
N2–C11	1.342(4)	C11–N3	1.334(5)
N2–C10	1.305(5)	N1–C10	1.328(4)
N1–C9	1.452(5)		
Cl1–Hg–Cl2	108.77(5)	Cl1–Hg–Te	115.15(3)
Cl1–Hg–S	102.73(4)	Cl2–Hg–Te	102.18(3)
Cl2–Hg–S	108.92(5)	Te–Hg–S	119.47(3)
Hg–S–C11	100.6(1)	S–C11–N2	120.3(3)
S–C11–N3	121.0(3)	C11–N2–C10	123.3(3)
N2–C10–N1	119.6(3)	C10–N1–C9	124.2(3)

Despite the fact that the nitrogen atom N2 does not contribute to the coordination of the metal, there is some π-electron delocalization observed in the backbone of the organic ligand, as is evident from bond length considerations (N2–C10/C11: 1.305/1.342 Å, N1–C9/C10: 1.452/1.328 Å). Such behavior is not unusual even for uncoordinated thiocarbamoylbenzamidines and has been reported before for other tridentate ligands of this class.[40,41]

Long-range interactions between tellurium and sulfur assemble each two molecules of **13** in the solid-state structure of the compound (see Figure 7, b). The corresponding distance of 3.4717(4) Å is within the sum of the van der Waals radii of sulfur and tellurium. Although a large number of weak Te···halide interactions have been discussed as the main factor for supramolecular arrangements of tellurium compounds,[30–34] the role of the corresponding Te···S contacts has hitherto been relatively less regarded.[42]

Conclusions

Telluroethers with accompanying picolinamido or thiocarbamoylbenzamidinato coordination sites are suitable ligands for the coordination of "soft" metal ions such as Pt^{2+}, Pd^{2+}, or Hg^{2+}. The resulting complexes aggregate through the formation of different kinds of long-range interactions between the tellurium atoms and the transition-metal ions, halido ligands, or sulfur atoms of adjacent molecules, which assemble them to dimeric or supramolecular arrangements. The nature of such aggregation of the molecules mainly influences the solid-state structures of such compounds. This demonstrates further that more knowledge is required to clarify the factors that allow control to be gained over structural details and, with this, over the chemical and physical properties of tellurium compounds with potential for applications in molecular and material science.

Experimental Section

Materials: All chemicals were reagent grade and used without further purification. Solvents were dried and freshly distilled prior to use, unless otherwise stated. 3-(Phenyltellanyl)propylammonium chloride, 2-picolinoyl chloride, and *N*-[*N′*,*N′*-methyl(phenyl)aminothiocarbonyl]benzimidoyl chloride were synthesized by following reported procedures.[43–45]

Physical Measurements: Infrared spectra were measured for KBr pellets with a Shimadzu FTIR spectrometer IRAffinity-1 between 400 and 4000 cm^{-1}. ESI^{+} mass spectra were recorded with an Agilent 6210 ESI–TOF (Agilent Technologies) instrument. All results are given in the form: *m*/*z*, assignment. Elemental analyses were determined with a Heraeus Vario El III elemental analyzer. NMR spectra were recorded with a JEOL 400 MHz multinuclear spectrometer. TMS (^{1}H, ^{13}C NMR), Me_2Te (^{125}Te NMR), $Na_2[PtCl_6]$ (^{195}Pt NMR), and Me_2Hg (^{199}Hg NMR) were used as external standards.

Syntheses of Ligands

HL1: Freshly prepared 2-picolinic acid chloride (398 mg, 3.23 mmol) was suspended in anhydrous MeCN (60 mL) and treated with NEt_3 (0.5 mL, 6.46 mmol). Solid 3-(phenyltellanyl)propylammonium chloride (850 mg, 3.23 mmol) was added and the resulting green reaction mixture was stirred for 3 h at room temperature. The solvent was removed under reduced pressure and the crude residue was redissolved in $CHCl_3$ (100 mL), and washed with distilled water (50 mL) and brine (100 mL). The combined organic layers were dried with anhydrous $MgSO_4$ and the solvent was removed under reduced pressure to yield a dark-brown viscous liquid. Purification was done by column chromatography using silica as stationary phase ($CHCl_3$/MeOH, 95:5). The product HL1 was obtained as a yellow-brown viscous oil and was finally dried under high vacuum, yield 75% (893 mg). $C_{15}H_{16}N_2OTe$ (367.90): calcd. C 48.9, H 4.4, N 7.6; found C 47.6, H 4.5, N 7.0. IR: $\tilde{\nu}$ = 3381 (s), 3053 (m), 2930 (s), 2860 (m), 1670 (s), 1589 (m), 1524 (s), 1464 (s), 1433 (s), 1364 (w), 1288 (m), 1246 (m), 1167 (m), 1088 (w), 1063 (w), 1042 (w), 1018 (m), 997 (s), 820 (m), 733 (s), 692 (s), 621 (m), 455 (m) cm^{-1}. ^1H NMR ($CDCl_3$): δ = 2.10 (quint, J = 7.6 Hz, 2 H, CH_2), 2.91 (t, J = 7.6 Hz, 2 H, Te-CH_2), 3.52 (q, J = 6.6 Hz, 2 H, N-CH_2), 7.15–7.19 (m, 2 H), 7.23–7.27 (m, 1 H), 7.39 (ddd, J = 7.6, 4.8, 1.2 Hz, 1 H), 7.70–7.73 (m, 2 H), 7.81 (td, J = 7.7, 1.7 Hz, 1 H, Ph, py), 8.07 (br. s, 1 H, NH), 8.16 (dt, J = 7.8, 1.0 Hz, 1 H, py), 8.50 (ddd, J = 4.8, 1.7, 0.9 Hz, 1 H, py) ppm. ^{13}C NMR ($CDCl_3$): δ = 4.9 (Te-CH_2), 31.7 (CH_2), 40.9 (N-CH_2), 111.4 (Te-Ph), 122.1 (py), 126.1 (py), 127.6 (Ph), 129.1 (Ph), 137.3 (Ph), 138.3 (py), 147.9 (py), 149.7 (py), 164.3 (C=O) ppm. ^{125}Te NMR ($CDCl_3$): δ = 483 ppm. MS (ESI$^+$, CH_2Cl_2/MeOH): m/z (%) = 409.00 (13) $[M + K]^+$, 393.02 (100) $[M + Na]^+$, 163.09 (50) $[M - TePh]^+$. HRMS: m/z calcd. for $[M + Na]^+$ 393.02175; found 393.0222.

HL2: A solution of *N*-[*N*′,*N*′-methyl(phenyl)aminothiocarbonyl]-benzimidoyl chloride (1 g, 3.46 mmol) in anhydrous acetone (10 mL) was added dropwise to a mixture of 3-(phenyltellanyl)-propylammonium chloride (910 mg, 3.46 mmol) and NEt_3 (1 mL, 7 mmol) in anhydrous acetone (5 mL). The color of the reaction mixture changed from yellow to dark red. Stirring was continued for 2 h at room temperature. After the suspension was cooled to 0 °C, a colorless precipitate of NEt_3·HCl was filtered off and the solvent was removed under reduced pressure. The residue was redissolved in CH_2Cl_2 (5 mL), washed with brine (3 × 5 mL) and the solvent was removed again under reduced pressure. The remaining dark-brown viscous liquid was purified by column chromatography using silica as stationary phase (CH_2Cl_2). After drying under high vacuum, the product HL2 was obtained as a dark-red viscous oil, yield 61% (1.09 g). $C_{24}H_{25}N_3STe$ (515.14): calcd. C 55.9, H 4.9, N 8.1, S 6.2; found C 52.9, H 4.7, N 7.1, S 6.3. IR: $\tilde{\nu}$ = 3298 (w), 3061 (w), 2926 (w), 1598 (s), 1574 (s), 1533 (w), 1493 (s), 1464 (w), 1433 (s), 1362 (s), 1333 (s), 1294 (s), 1134 (w), 1099 (s), 1018 (w), 997 (w), 903 (w), 775 (w), 733 (m), 694 (s), 563 (w), 528 (w), 453 (w) cm^{-1}. ^1H NMR ($CDCl_3$): δ = 1.83–2.01 (m, 2 H, CH_2), 2.70–2.83 (m, 2 H, Te-CH_2), 3.25–3.34 (m, 2 H, N-CH_2), 3.54–3.63 (m, 3 H, CH_3), 7.01–7.44 (m, 13 H, Ph), 7.65 (d, J = 7.2 Hz, 2 H, Ph), 10.22 (s, 1 H, NH) ppm. ^{13}C NMR ($CDCl_3$): δ = 5.8 (Te-CH_2), 29.8 (CH_2), 43.7 (N-CH_2), 53.7 (CH_3), 112.4 (Te-Ph), 126.0, 126.3, 126.4, 127.0, 127.7, 127.9, 128.1, 128.5, 129.0, 129.3, 129.4, 129.5, 129.9, 130.6, 134.6, 138.5 (Ph), 145.1 (N-Ph), 155.8 (C=N), 190.1 (C=S) ppm. ^{125}Te NMR ($CDCl_3$): δ = 471, 475 (*E*/*Z* isomers) ppm. MS (ESI$^+$, CH_2Cl_2/MeOH): m/z (%) = 1069.12 (9) $[2M + K]^+$, 1053.15 (55) $[2M + Na]^+$, 556.05 (8) $[M + K]^+$, 540.07 (47) $[M + Na]^+$, 516.08 (100) $[M + H]^+$. HRMS: m/z calcd. for $[M + H]^+$ 516.0745; found 516.0765.

Synthesis of Complexes

[MCl(L1-κ*N*,*N*′,*Te*)] [M = Pt (7), Pd (8)]: A suspension of HL1 (37 mg, 0.1 mmol) in CH_2Cl_2 (3 mL) was added dropwise to a stirred suspension of MCl_2 [27 mg (**7**), 18 mg (**8**), 0.1 mmol] in MeOH (3 mL). The temperature of the reaction mixtures was kept at 30 °C for 1 h, whereupon clear solutions were formed. The CH_2Cl_2 was evaporated and brownish-yellow solids started to precipitate. The solids were filtered off, washed with a small amount of cold MeOH, and dried in high vacuum, yields of the noncrystalline products: 66% (39 mg) (**7**) and 77% (28 mg) (**8**). Orange-red single crystals suitable for X-ray diffraction analysis were obtained by recrystallization from CH_2Cl_2/MeOH (v/v 1:1) (**7** and **8**) or DMSO (**7**).

Data for 7 (M = Pt): $C_{15}H_{15}ClN_2OPtTe$ (597.44): calcd. C 30.2, H 2.5, N 4.7; found C 30.1, H 2.5, N 4.5. IR: $\tilde{\nu}$ = 3049 (w), 2924 (w), 2846 (w), 1622 (s), 1595 (s), 1476 (w), 1437 (w), 1377 (w), 1281 (w), 1250 (w), 1177 (w), 1096 (w), 1051 (w), 997 (w), 758 (w), 733 (w), 689 (w), 679 (w), 544 (w), 478 (w), 453 (w) cm^{-1}. ^1H NMR ($CDCl_3$): δ = 2.13–2.22 (m, 1 H, CH_2), 2.48 (qd, J = 9.3, 5.4 Hz, 2 H, Te-CH_2), 2.75–2.83 (m, 1 H, CH_2), 3.20 (dd, J = 14.7, 9.7 Hz, 1 H, N-CH_2), 3.78 (ddd, J = 13.0, 8.1, 5.1 Hz, 1 H, N-CH_2), 7.31–7.35 (m, 2 H), 7.39–7.43 (m, 1 H), 7.56 (ddd, J = 7.3, 5.6, 1.5 Hz, 1 H), 7.86–7.88 (m, 1 H), 8.02 (dt, J = 7.7, 1.4 Hz, 1 H), 8.07 (tt, J = 5.3, 2.2 Hz, 2 H, Ph, py), 9.20–9.21 (m, 1 H, py) ppm. ^{13}C NMR ([D_6]DMSO): δ = 14.9 (Te-CH_2), 32.2 (CH_2), 45.5 (N-CH_2), 116.7 (Te-Ph), 125.7, 128.0, 129.8, 130.2, 137.4, 141.7 (Ph, py), 144.5 (py), 152.4 (py), 172.3 (C=O) ppm. ^{125}Te NMR ([D_6]DMSO): δ = 537 ($J|^{195}Pt^{125}Te|$ = 3215 Hz) ppm. ^{195}Pt NMR ([D_6]DMSO): δ = –3450 ppm. MS (ESI$^+$, CH_2Cl_2/MeOH): m/z (%) = 1815.85 (8) $[3M + Na]^+$, 1218.90 (22) $[2M + Na]^+$, 638.94 (9) $[M + K]^+$, 620.94 (100) $[M + Na]^+$, 598.96 (8) $[M + H]^+$, 562.98 (9) $[M - Cl]^+$, 484.94 (14) $[M - py, - Cl]^+$. HRMS: m/z calcd for $[M + Na]^+$ 620.9402; found 620.9444.

Data for 8 (M = Pd): $C_{15}H_{15}ClN_2OPdTe$ (508.75): calcd. C 35.4, H 3.0, N 5.5; found C 35.0, H 3.1, N 5.4. IR: $\tilde{\nu}$ = 3069 (w), 3044 (w), 2994 (w), 2926 (w), 2849 (w), 1611 (s), 1585 (s), 1570 (s), 1474 (w), 1433 (w), 1373 (m), 1358 (m), 1283 (w), 1248 (w), 1171 (w), 1138 (w), 1092 (w), 1049 (w), 997 (w), 935 (w), 806 (w), 781 (w), 756 (m), 735 (m), 689 (m), 655 (w), 542 (w), 509 (w), 473 (w), 449 (w), 407 (w) cm^{-1}. ^1H NMR ($CDCl_3$): δ = 2.06–2.16 (m, 1 H, CH_2), 2.46–2.57 (m, 2 H, Te-CH_2), 2.65–2.71 (m, 1 H, CH_2), 3.02 (dd, J = 14.7, 9.7 Hz, 1 H, N-CH_2), 3.62 (dd, J = 14.8, 6.9 Hz, 1 H, N-CH_2), 7.33–7.37 (m, 2 H), 7.41–7.45 (m, 1 H), 7.50 (ddd, J = 7.2, 5.4, 1.6 Hz, 1 H), 7.92 (dd, J = 7.8, 1.5 Hz, 1 H), 7.98 (td, J = 7.6, 1.5 Hz, 2 H), 8.09–8.12 (m, 2 H, Ph, py), 8.93–8.95 (m, 1 H, py) ppm. ^{13}C NMR ([D_6]DMSO): δ = 15.3 (Te-CH_2), 32.2 (CH_2), 45.2 (N-CH_2), 118.1 (Te-Ph), 125.4, 127.6, 130.0, 130.1, 137.6, 141.6 (Ph, py), 146.1 (py), 153.8 (py), 172.2 (C=O) ppm. ^{125}Te NMR ([D_6]DMSO): δ = 577 ppm. MS (ESI$^+$, CH_2Cl_2/MeOH): m/z (%) = 1564.66 (6) $[3M + K]^+$, 1548.68 (31) $[3M + Na]^+$, 1094.84 (6) $[2M - H, + 2K]^+$, 1056.76 (21) $[2M + K]^+$, 1040.78 (46) $[2M + Na]^+$, 982.83 (34) $[2M - Cl]^+$, 586.94 (11) $[M + 2K]^+$, 548.86 (26) $[M + K]^+$, 532.89 (55) $[M + Na]^+$, 510.91 (13) $[M + H]^+$, 474.93 (100) $[M - Cl]^+$, 446.90 (35) $[M - Cl, - (CO)]^+$. HRMS: m/z calcd. for $[M + Na]^+$ 532.8867; found 532.8875.

[PtI_3(L1-κ*N*,*N*′,*Te*)] (9): A solution of HL1 (37 mg, 0.1 mmol) in CH_2Cl_2 (2 mL) was added dropwise to a stirred suspension of $PtCl_2$ (27 mg, 0.1 mmol) in MeOH (2 mL). The reaction mixture was heated to reflux until a brown precipitate of complex **7** was formed. The suspension was treated with a solution of iodine (50 mg, 0.2 mmol) in methanol (1 mL) and stirred for a further 5 min at room temperature. Finally, the solvent was removed and the solid was recrystallized from CH_2Cl_2/$CHCl_3$/MeOH (v/v/v 1.5:4:1.5). Slow evaporation on air gave black blocks, yield 75% (71 mg). $C_{15}H_{15}I_3N_2OPtTe$ (942.70): calcd. C 19.1, H 1.6, N 3.0; found C 19.1, H 1.6, N 2.9. IR: $\tilde{\nu}$ = 3051 (w), 2980 (w), 2924 (w), 2851 (w), 1670 (w), 1638 (w), 1612 (m), 1582 (s), 1568 (s), 1520 (w), 1474 (w), 1431 (m), 1406 (m), 1383 (m), 1304 (w), 1292 (w), 1277 (w), 1250 (m), 1192 (w), 1171 (w), 1144 (w), 1092 (w), 1045 (w), 1030 (m), 1000 (m), 996 (w), 934 (w), 779 (w), 754 (m), 735 (s), 677 (m), 654 (m), 538 (w), 449 (w) cm^{-1}. ^1H NMR ($CDCl_3$): δ = 2.90–3.39 (m, 4 H, CH_2, Te-CH_2), 3.63–3.84 (m, 1 H, N-CH_2), 3.95–4.16 (m, 1

H, N-CH_2), 7.34–7.90 (m, 4 H), 8.07 (d, J = 7.6 Hz, 1 H), 8.16 (dd, J = 16.0, 7.2 Hz, 2 H), 8.49–8.76 (m, 1 H, Ph, py), 9.78 (d, J = 5.0 Hz, 1 H, py) ppm. ^{13}C NMR ([D$_6$]DMSO): δ = 15.1 (Te-CH_2), 26.4, 26.7 (CH_2), 44.2 (N-CH_2), 117.5 (Te-Ph), 122–138 (Ph, py), 148–150 (py), 164.7 (C=O) ppm. ^{125}Te NMR ([D$_6$]DMSO): δ = 973 ppm. ^{195}Pt NMR ([D$_6$]DMSO): δ = 2367 ppm.

[$PdI_2(PhTeI)_2$] (10): HL1 (37 mg, 0.1 mmol) dissolved in CH_2Cl_2 (2 mL) was added dropwise to a stirred suspension of $PdCl_2$ (18 mg, 0.1 mmol) in MeOH (2 mL). The reaction mixture was heated to reflux and treated with a solution of iodine (50 mg, 0.2 mmol) in MeOH/CH_2Cl_2 (4:1 v/v, 2.5 mL). The resulting solution was stirred for a further 5 min at 35 °C, followed by evaporation of the solvent. The remaining oily residue was redissolved in a mixture of CH_2Cl_2/$CHCl_3$/MeOH (1.5:4:1.5 v/v/v) and kept for crystallization. A small amount of black plates crystallized within one week. Complete evaporation of the mixture again gave an unattractive brown oil, which was finally discarded, yield 3 mg (6%). $C_{12}H_{10}I_4PdTe_2$ (1023.43): calcd. C 14.1, H 1.0; found C 15.6, H 1.4. IR: $\tilde{\nu}$ = 3044 (w), 1568 (w), 1508 (w), 1470 (m), 1431 (m), 1325 (w), 1304 (w), 1292 (w), 1177 (w), 1153 (w), 1051 (w), 1013 (w), 995 (m), 800 (w), 731 (s), 683 (s), 447 (w) cm^{-1}. ^1H NMR ([D$_6$]DMSO): δ = 6.67–8.47 (m, 10 H, Ph) ppm.

[MCl(L2-κ*S*,*N*,*Te*)] [M = Pt (11), Pd (12)]: HL2 (52 mg, 0.1 mmol) was dissolved in CH_2Cl_2 (2 mL) and added dropwise to a stirred suspension of MCl_2 [27 mg (**11**), 18 mg (**12**), 0.1 mmol] in MeOH (2 mL). The reaction mixture was heated to reflux for 1.5 h and the solvent was removed. The initially crude viscous residue solidified to a brown (**11**) or dark brown (**12**) powder by repeated treatments with diethyl ether. The solid was washed with Et_2O and dried in high vacuum, yield 72 mg (95%) (**11**) and 62 mg (97%) (**12**).

Data for 11 (**M = Pt**): $C_{24}H_{24}ClN_3PtSTe$ (744.68): calcd. C 38.7, H 3.3, N 5.6; found C 40.6, H 4.1, N 5.6. IR: $\tilde{\nu}$ = 3048 (w), 2924 (w), 2853 (w), 1599 (m), 1568 (m), 1539 (s), 1489 (s), 1474 (m), 1435 (s), 1404 (w), 1398 (w), 1373 (w), 1296 (w), 1261 (w), 1177 (w), 1159 (w), 1111 (w), 1094 (w), 1070 (w), 1016 (w), 997 (w), 800 (w), 768 (w), 735 (m), 692 (s), 557 (w), 453 (w) cm^{-1}. ^1H NMR ([D$_6$]DMSO): δ = 1.46–2.55 (m, 4 H, CH_2, Te-CH_2), 3.09–3.96 (m, 5 H, N-CH_2, CH_3), 6.90–8.11 (m, 15 H, Ph) ppm. ^{13}C NMR ([D$_6$]DMSO): δ = 9.0 (Te-CH_2), 28.9 (CH_2), 45.9 (N-CH_2), 52.8 (CH_3), 115.3 (Te-Ph), 123–141 (Ph), 145.4 (N-Ph), 170.7 (C=N), 189.8 (C=S) ppm. ^{125}Te NMR ($CDCl_3$): δ = 515 ($J|^{195}Pt^{125}Te|$ = 2303 Hz) ppm. ^{195}Pt NMR ([D$_6$]DMSO): δ = –3663, –3792 ppm. MS (ESI$^+$, CH_2Cl_2/MeOH): m/z (%) = 1532.05 (1) [2M – Cl, + 2K]$^+$, 1525.00 (1) [2M + Cl]$^+$, 1491.02 (17) [2M + 2H]$^+$, 1455.04 (2) [2M – Cl, + H]$^+$, 1077.07 (10) [2M – PtCl, – TePh, + Na]$^+$, 783.97 (1) [M + K]$^+$, 768.00 (1) [M + Na]$^+$, 746.01 (8) [M]$^+$, 710.04 (14) [M – Cl]$^+$, 105.04 (100) [$PhNCH_2$]$^+$. HRMS: m/z calcd. for [M]$^+$ 746.0089; found 746.0139.

Data for 12 (M = Pd): IR: $\tilde{\nu}$ = 3048 (w), 2963 (w), 2924 (w), 2859 (w), 1587 (s), 1545 (s), 1491 (s), 1474 (s), 1447 (s), 1435 (s), 1396 (m), 1368 (m), 1344 (m), 1302 (m), 1265 (m), 1157 (w), 1090 (m), 1070 (m), 1016 (m), 997 (m), 903 (w), 802 (w), 768 (w), 735 (m), 692 (s), 559 (m), 453 (w) cm^{-1}. ^1H NMR ($CDCl_3$): δ = 1.51–2.66 (m, 4 H, CH_2, Te-CH_2), 3.16–3.98 (m, 5 H, N-CH_2, CH_3), 6.89–8.53 (m, 15 H, Ph) ppm. ^{13}C NMR ([D$_6$]DMSO): δ = 9.2 (Te-CH_2), 28.9 (CH_2), 46.3 (N-CH_2), 52.8 (CH_3), 115.3 (Te-Ph), 123–141 (Ph), 145.0 (N-Ph), 170.0 (C=N), 189.8 (C=S) ppm. ^{125}Te NMR ([D$_6$]DMSO): δ = 539, 542 (*E*/*Z* isomers) ppm. MS (ESI$^+$, CH_2Cl_2/MeOH): m/z (%) = 1316.96 (1) [2M – Cl, + K]$^+$, 1276.92 (9) [2M – Cl]$^+$, 657.95 (11) [M + H]$^+$, 621.98 (39) [M – Cl]$^+$, 516.07 (15) [M – PdCl]$^+$, 206.94 (16) [PhTe]$^+$, 105.06 (100) [$PhNCH_2$]$^+$. HRMS: m/z calcd. for [M + H]$^+$ 657.9554; found 657.9513.

[$HgCl_2$(HL2-κ*S*,*Te*)] (13): A solution of HL2 (52 mg, 0.1 mmol) in CH_2Cl_2/MeOH (1:1 v/v, 1 mL) was added dropwise to a stirred solution of $HgCl_2$ (27 mg, 0.1 mmol) in MeOH (1 mL). A brownish precipitate formed immediately. The reaction mixture was stirred for a further 20 min at room temperature. The solid was filtered off, washed with MeOH and dried in high vacuum, yield of the noncrystalline product: 84% (66 mg). Colorless single crystals suitable for X-ray diffraction analysis were obtained by recrystalli-

Table 5. Crystal data and details of the structure determinations.

	[PtCl(L1-κ*N*,*N*′,*Te*)]	[PdCl(L1-κ*N*,*N*′,*Te*)]$_4$· MeOH·1/2 H_2O	[PtI_3(L1-κ*N*,*N*′,*Te*)]· 3/2 H_2O	[$PdI_2(PhTeI)_2$]	[$HgCl_2$(HL2-κ*S*,*Te*)]· 1/8 H_2O
Formula	$C_{15}H_{15}ClN_2OPtTe$	$C_{61}H_{65}Cl_4N_8O_{5.5}Pd_4Te_4$	$C_{15}H_{15}I_3N_2O_{2.5}PtTe$	$C_{12}H_{10}I_4PdTe_2$	$C_{24}H_{25}Cl_2N_3O_{0.125}STeHg$
M_w	597.43	2076.01	944.68	1023.40	788.62
Crystal system	monoclinic	triclinic	monoclinic	orthorhombic	triclinic
a [Å]	10.654(2)	14.700(2)	12.447(1)	47.189(1)	9.675(1)
b [Å]	15.693(2)	17.132(2)	13.714(1)	16.871(2)	12.197(1)
c [Å]	9.927(2)	18.545(2)	14.013(2)	9.784(4)	13.503(1)
α [°]	90	114.27(1)	90	90	90.52(1)
β [°]	108.61(1)	107.55(1)	109.28(1)	90	104.84(1)
γ [°]	90	109.59(1)	90	90	111.62(1)
V [Å^3]	1572.9(5)	3446.6(7)	2257.8(4)	7786(3)	1422.4(2)
Space group	$P2_1/c$	$P\bar{1}$	$P2_1/n$	$Fdd2$	$P\bar{1}$
Z	4	2	4	16	2
$D_{calcd.}$ [g cm^{-3}]	2.523	2.000	2.844	3.492	1.841
μ [mm^{-1}]	10.907	2.894	11.596	10.222	6.693
Abs. correction	integration	integration	SADABS	integration	SADABS
$T_{min.}$	0.3321	0.3495	0.1847	0.1849	0.0976
$T_{max.}$	0.6197	0.8688	0.3619	0.2783	0.6165
Reflections	10414	40701	51089	5703	42613
Independent refl.	4223	18471	4616	3697	8705
Parameters	190	805	214	172	299
$R1/wR2$	0.0345/0.0493	0.0438/0.0939	0.0442/0.1321	0.0286/0.0583	0.0261/0.0979
GOF	0.842	0.880	1.024	0.911	1.327
CCDC number	CCDC-1053765	CCDC-1053766	CCDC-1053767	CCDC-1053768	CCDC-1053769

zation from DMSO. $C_{24}H_{25}Cl_2HgN_3STe$ (786.64): calcd. C 36.6, H 3.2, N 5.3, S 4.1; found C 33.6, H 3.1, N 4.5, S 4.0. IR: $\tilde{\nu}$ = 3254 (w), 3107 (w), 3051 (w), 2926 (w), 1585 (m), 1549 (s), 1491 (m), 1476 (m), 1443 (m), 1398 (w), 1369 (w), 1346 (w), 1300 (m), 1240 (w), 1173 (w), 1094 (m), 1072 (w), 997 (w), 874 (w), 849 (w), 768 (w), 731 (m), 689 (m), 559 (w), 527 (w), 457 (w) cm^{-1}. ^1H NMR ($[D_6]$DMSO): δ = 1.71–2.60 (m, 4 H, CH_2, Te-CH_2), 2.82–3.58 (m, 5 H, N-CH_2, CH_3), 6.78–7.92 (m, 15 H, Ph), 10.65 (s, 1 H, NH) ppm. ^{13}C NMR ($[D_6]$DMSO): δ = 19.5 (Te-CH_2), 29.2 (CH_2), 44.2, 43.6 (N-CH_2), 55.5 (CH_3), 115.6 (Te-Ph), 126.3, 126.8, 127.7, 128.8, 128.9, 129.3, 129.7, 130.2, 130.3, 132.7, 132.9, 137.8, 139.4 (Ph), 145.0 (N-Ph), 161.2 (C=N), 184.2 (C=S) ppm. ^{125}Te NMR ($[D_6]$DMSO): δ = 393, 398 ppm. ^{199}Hg NMR ($[D_6]$DMSO): δ = –1227 ppm. MS (ESI^+, CH_2Cl_2): *m/z* (%) = 1301.09 (2) $[2M - HgCl_2]^+$, 1267.11 (4) $[2M - HgCl_2, - Cl]^+$, 850.17 (9) $[M + H, + Na, + K]^+$, 818.14 (11) $[M - 2Cl, + Na, + K]^+$, 774.21 (1) $[M - HCl, + Na]^+$, 752.03 (1) $[M - Cl]^+$, 516.09 (7) $[M - HgCl_2, - H]^+$.

X-ray Crystallography: The intensities for the X-ray determinations were collected with a STOE IPDS 2T instrument {$[PtCl(L1\text{-}\kappa N,N',Te)]$, $[PdCl(L1\text{-}\kappa N,N',Te)]_4\cdot MeOH\cdot 1/2\ H_2O$ and $[PdI_2(PhTeI)_2]$} at *T* = 200 K and with a BRUKER Apex II ($[PtI_3(L1\text{-}\kappa N,N',Te)]\cdot 3/2H_2O$ and $[HgCl_2(HL2\text{-}\kappa S,Te)]\cdot 1/8H_2O$) with Mo-$K_\alpha$ radiation (λ = 0.71073 Å) at 296 K. Standard procedures were applied for data reduction and absorption correction. Structure solution and refinement were performed with SHELXS-97 and SHELXL-97.[46] Hydrogen atom positions were calculated for idealized positions and treated with the "riding model" option of SHELXL. More details on data collections and structure calculations are contained in Table 5. Additional information on the structure determinations have been deposited with the Cambridge Crystallographic Data Centre (Cambridge, UK).

The CCDC numbers given in Table 5 contain the supplementary crystallographic data for this paper. These data can be obtained free of charge from The Cambridge Crystallographic Data Centre via www.ccdc.cam.ac.uk/data_request/cif.

Computational Details: Density functional theory calculations were performed using the Gaussian code.[47] The hybrid B3LYP functional[48,49] was used to describe the exchange and correlation functional. We used the CEP-321G split-valence effective core potential basis set for the light (H, C, and O) atoms, and the all electron split valence 6-31G basis set, augmented with (d,p) polarization functions, for the heavy (Pd, Te, and I) atoms. The electron localization function was calculated by using the Dgrid code,[50] and its contour map was constructed by using the Chemcraft software.[51] Bader analysis was performed by using the aim-uc code.[52]

Supporting Information (see footnote on the first page of this article): ^{13}C NMR and ESI mass spectra; computational details.

Acknowledgments

This work was generously supported by the German Deutscher Akademischer Austauschdienst (DAAD) and the Brazilian Coordenação de Aperfeiçoamento de Pessoal de Nível Superior (CAPES) under the program CAPES-PROBRAL. The calculations have been performed using the computational facilities of CPAD/UFSM.

---

[1] F. A. Christy, P. S. Shrivastav, *Crit. Rev. Anal. Chem.* **2011**, *41*, 236–269.

[2] H. Tsukube, *Coord. Chem. Rev.* **1996**, *148*, 1–17.

[3] S. G. Murray, F. G. Hartley, *Chem. Rev.* **1981**, *81*, 365–414.

[4] W. Levason, S. D. Orchard, G. Reid, *Coord. Chem. Rev.* **2002**, *225*, 159–199.

[5] W. Levason, G. Reid, W. Zhang, *Dalton Trans.* **2011**, *40*, 8491–8506.

[6] A. K. Singh, S. Sharma, *Coord. Chem. Rev.* **2000**, *209*, 49–98.

[7] J.-K. Shen, J.-C. Gao, Q.-Z. Shi, F. Rheingold, F. Basolo, *Inorg. Chem.* **1991**, *30*, 1868–1873.

[8] K. Badyal, W. R. McWhinnie, H. L. Chen, T. A. Hamor, *J. Chem. Soc., Dalton Trans.* **1997**, 1579–1585.

[9] W. Levason, S. D. Orchard, G. Reid, *Organometallics* **1999**, *18*, 1275–1280.

[10] E. G. Hope, *Coord. Chem. Rev.* **1993**, *122*, 109–170.

[11] V. Srivastava, A. K. Singh, B. L. Khandelwal, *Transit. Met. Chem.* **1992**, *17*, 177–180.

[12] A. Khalid, A. K. Singh, *J. Coord. Chem.* **1996**, *39*, 313–320.

[13] A. Singh, *Proc. Indian Acad. Sci. Chem. Sci.* **2002**, *114*, 357–366.

[14] A. K. Singh, V. Srivastava, *J. Coord. Chem.* **1992**, *27*, 237–253.

[15] R. Batheja, S. K. Dhingra, A. K. Singh, *J. Organomet. Chem.* **1995**, *487*, 173–176.

[16] K. P. Raghavendra, A. K. Singh, R. J. Butcher, P. Sharma, R. A. Toscano, *Eur. J. Inorg. Chem.* **2004**, 1107–1114.

[17] A. Kumar, M. Agarwal, A. K. Singh, R. J. Butcher, *Inorg. Chim. Acta* **2009**, *362*, 3208–3218.

[18] K. P. Raghavendra, A. K. Singh, J. E. Drake, M. B. Hursthouse, M. E. Little, *Struct. Chem.* **2007**, *18*, 203–207.

[19] P. P. Raghavendra, G. Singh, S. Bali, A. K. Singh, *Phosphorus Sulfur Silicon Relat. Elem.* **2005**, *180*, 903–911.

[20] N. Kumar, M. S. Milton, J. D. Singh, S. Upreti, R. J. Butcher, *Tetrahedron Lett.* **2006**, *47*, 885–889.

[21] P. Khandelwal, T. P. Kaur, J. D. Singh, B. L. Khandelwal, *Indian J. Chem. Sect. A* **1997**, *36*, 1086–1090.

[22] G. Singh, A. K. Singh, P. Sharma, J. E. Drake, M. B. Hursthouse, M. E. Light, *J. Organomet. Chem.* **2003**, *688*, 20–26.

[23] A. Khalid, A. K. Singh, *J. Coord. Chem.* **1996**, *39*, 313–320.

[24] V. Srivastava, A. K. Singh, B. L. Khandelwal, *Transit. Met. Chem.* **1992**, 177–180.

[25] V. K. Jain, S. Chaudhury, R. Bohra, *Polyhedron* **1993**, *12*, 2377–2385.

[26] S. Bali, A. K. Singh, P. Sharma, R. A. Toscano, J. E. Drake, M. B. Hursthouse, M. E. Light, *J. Organomet. Chem.* **2004**, *689*, 2346–2353.

[27] A. Singh, *Proc. Indian Acad. Sci. Chem. Sci.* **2002**, *114*, 357–366.

[28] K. Brandenburg, *DIAMOND*, v. 3.2i, Crystal Impact GbR, Bonn, Germany.

[29] I. Haiduc, J. Zukerman-Schpector, *Phosphorus Sulfur Silicon Relat. Elem.* **2001**, *171*, 171–185.

[30] J. Zukerman-Schpector, I. Haiduc, R. L. Camillo, J. V. Comasseto, R. L. O. R. Cunha, A. Jorge, *Can. J. Chem.* **2002**, *80*, 1530–1537.

[31] P. C. Srivastava, S. Bajpai, R. Lath, S. M. Bajpai, R. Kumar, R. J. Butcher, *Polyhedron* **2004**, *23*, 1629–1639.

[32] A. F. Cozzolino, P. J. W. Elder, I. Vargas-Baca, *Coord. Chem. Rev.* **2011**, *255*, 1426–1438.

[33] A. Alvarez-Larena, J. Farran, J. F. Piniella, *Supramolecular Arrangements in Organotellurium Compounds via Te···Halogen Contacts*, in: *Current Trends in X-ray Crystallography* (Ed.: A. Chandrasekaran), Intechopen.com, **2011**, chapter 5; DOI: 10.5772/30097.

[34] E. S. Lang, R. M. Fernandes Jr., E. T. Silveira, U. Abram, E. M. Vazquez-Lopez, *Z. Anorg. Allg. Chem.* **1999**, *625*, 1401–1404.

[35] P. D. Boyle, W. I. Cross, S. M. Godfrey, C. A. McAuliffe, R. G. Pritchard, S. Sawar, J. M. Sheffield, *Angew. Chem. Int. Ed.* **2000**, *39*, 1796–1798; *Angew. Chem.* **2000**, *112*, 1866.

[36] E. S. Lang, G. N. Ledesma, U. Abram, M. Vega-Teijido, I. Caracelli, J. Zukerman-Schpector, *Z. Kristallogr.* **2006**, *221*, 166–172.

[37] O. Vicane, *Acta Chem. Scand., Ser. A* **1975**, *29*, 787–793.

[38] Y. Torubaev, A. Pasynskii, P. Mathur, *J. Organomet. Chem.* **2009**, *694*, 1781–1785.
[39] Y. Torubaev, A. Pasynskii, P. Mathur, *Koord. Khim.* **2008**, *34*, 807–811.
[40] N. H. Huy, J. Grewe, J. Schroer, B. Kuhn, U. Abram, *Inorg. Chem.* **2008**, *47*, 5136–5144.
[41] H. H. Nguyen, J. J. Jegathesh, P. I. da S. Maia, V. M. Deflon, R. Gust, S. Bergemann, U. Abram, *Inorg. Chem.* **2009**, *48*, 9356–9364.
[42] E. R. T. Tiekink, J. Zukerman-Schpector, *Coord. Chem. Rev.* **2010**, *254*, 46–76.
[43] A. Khanna, A. Bala, B. L. Khandelwal, *J. Organomet. Chem.* **1995**, *494*, 199–204.
[44] J. M. Rowland, M. L. Thornton, M. M. Olmstead, P. K. Mascharak, *Inorg. Chem.* **2001**, *40*, 1069–1073.
[45] L. Beyer, R. Widera, *Tetrahedron Lett.* **1982**, *23*, 1881–1882.
[46] G. M. Sheldrick, *SHELXS-97 and SHELXL-97 – Programs for the solution and refinement of X-ray crystal structures*, University of Göttingen, Germany, **1997**.
[47] M. J. Frisch, G. W. Trucks, H. B. Schlegel, G. E. Scuseria, M. A. Robb, J. R. Cheeseman, G. Scalmani, V. Barone, B. Mennucci, G. A. Petersson, H. Nakatsuji, M. Caricato, X. Li, H. P. Hratchian, A. F. Izmaylov, J. Bloino, G. Zheng, J. L. Sonnenberg, M. Hada, M. Ehara, K. Toyota, R. Fukuda, J. Hasegawa, M. Ishida, T. Nakajima, Y. Honda, O. Kitao, H. Nakai, T. Vreven, J. A. Montgomery Jr., J. E. Peralta, F. Ogliaro, M. Bearpark, J. J. Heyd, E. Brothers, K. N. Kudin, V. N. Staroverov, R. Kobayashi, J. Normand, K. Raghavachari, A. Rendell, J. C. Burant, S. S. Iyengar, J. Tomasi, M. Cossi, N. Rega, J. M. Millam, M. Klene, J. E. Knox, J. B. Cross, V. Bakken, C. Adamo, J. Jaramillo, R. Gomperts, R. E. Stratmann, O. Yazyev, A. J. Austin, R. Cammi, C. Pomelli, J. W. Ochterski, R. L. Martin, K. Morokuma, V. G. Zakrzewski, G. A. Voth, P. Salvador, J. J. Dannenberg, S. Dapprich, A. D. Daniels, O. Farkas, J. B. Foresman, J. V. Ortiz, J. Cioslowski, D. J. Fox, *Gaussian 09*, revision G09/2.2.4, Gaussian, Inc., Wallingford CT, **2009**.
[48] A. D. Becke, *J. Chem. Phys.* **1993**, *98*, 5648–5652.
[49] C. Lee, W. Yang, R. G. Parr, *Phys. Rev. B* **1988**, *37*, 785–789.
[50] M. Kohout, *DGrid*, v. 4.6, Radebeul, Germany, **2011**.
[51] *Chemcraft*, v. 1.8; available from http://www.chemcraftprog.com.
[52] D. Vega, D. Almeida, *J. Comput. Methods Sci. Eng.* **2014**, *14*, 131–136.

Received: April 2, 2015